9

Orthokinetic Stability of Food Emulsions

Siva A. Vanapalli
University of Michigan, Ann Arbor, Michigan, U.S.A.

John N. Coupland
The Pennsylvania State University, University Park, Pennsylvania, U.S.A.

I. INTRODUCTION

Many foods and food ingredients are oil-in-water emulsions. The functional properties of the emulsion depend on its microstructure, which is, in turn, controlled by the ingredients and processes used. Thus, it is useful to establish predictive links between (a) ingredients/process and microstructure and (b) microstructure and functionality. In the present context, our main concern is how shear, which is ubiquitous to almost all process operations, influences droplet aggregation (a microstructural feature) in emlusions.

There are very many mechanisms by which emlusions may break down, perhaps the most important are flocculation and, in the case of semicrystalline droplets, the related phenomenon of partial coalescence. Both mechanisms lead to the formation of extensive networks of droplets that can increase the viscosity of a product and lead to eventual coalescence and oiling-off (1). Flocculation can occur by a number of mechanisms and cause a wide range of changes in bulk functional properties, but in all cases, we can identify the fundamental event as two isolated droplets being held at a finite separation for a significant period of time. There must be a minimum in the interdroplet pair potential to hold the particles together, but to reach this separation, the droplets must first approach one

Table 1 Typical Shear Rates Encountered in Food Emulsions

Situation operation	Shear rate (s^{-1})
Creaming	10^{-6}–10^{-3}
Pouring	10^{-2}–10^2
Chewing and swallowing	10^1–10^2
Mixing and stirring	10^1–10^3
Pumping	10^0–10^3

Source: Adapted from Refs. 2 and 3.

another. It is here that applied shear forces have their greatest effect. Droplets encounter one another in a quiescent fluid through Brownian motion, but this rate may be increased by imposed movement in the fluid. Additionally, the kinetic energy of a particle may enable it to overcome local repulsion in the pair potential and allow droplets to aggregate, or the shear forces may rupture existing flocs. The relationships between applied flow and structure is further complicated by the fact that the structures formed and broken will, in turn, affect the emulsion viscosity and, hence, the rate of strain caused by an applied stress.

Despite the wide range of shear forces at all stages of food preparation and use (see Table 1) and their theoretical importance on emulsion stability, there have been very limited quantitative considerations of shear as a variable in the food science literature. This work is an attempt to summarize the basic theories of particle aggregation under shear in a format useful for food scientists and, second, to review some of the studies of the effects of shear on the stability of emulsions. Our major focus is on floc formation and fracture and we neglect the related topic of emulsion formation (see Ref. 4). We similarly neglect any treatment of the effects of emulsion structure on the shear properties of the bulk fluid [i.e., emulsion rheology (5)]. We begin by reviewing the fundamental Smoluchowski theory of colloidal aggregation and some of the more recent attempts to deal with its limitations. We next consider trajectory analysis, which is a complementary approach to Smoluchowski theory. Finally, we review some experimental studies on orthokinetic stability relevant to food emulsions.

II. THEORETICAL APPROACHES

The mechanism of aggregation involves two major steps: the *transport* step, leading to collision between two droplets, and the *attachment* step, in which the droplets stick to each other. Collisions occur due to local variations in
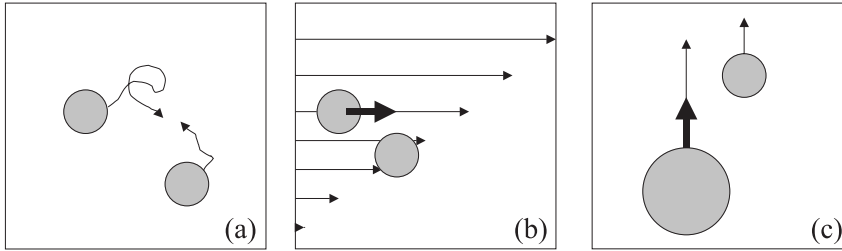
Figure 1 Various mechanisms of particle collision: (a) perikinetic, particles move by random Brownian motion and collide; (b) orthokinetic, particles move in a velocity gradient and the velocity difference between two particles leads to collision; (c) differential, particles cream at different rates because of their different sizes and the velocity gradient leads to a collision.

fluid/droplet velocities arising from (a) random thermal movement of droplets due to Brownian motion (*perikinetic* flocculation), (b) externally imposed velocity gradients from mixing (*orthokinetic* flocculation), and (c) differences in creaming velocities of individual droplets (*differential* flocculation) (Fig. 1). In general, for particle sizes $> 1\,\mu m$, perikinetic aggregation becomes less significant and orthokinetic aggregation predominates (6). For particle sizes $> 10\,\mu m$, differential flocculation becomes important (7).

The flux of particles through a collision surface is typically represented by the *collision frequency*. Because not all collisions lead to attachment, *collision efficiency* is used to describe the percentage of collisions that lead to aggregation. Collision efficiency is governed by the interdroplet potential arising from the sum of colloidal and hydrodynamic interactions. The rate of droplet flocculation (J) can be taken as the product of a collision rate and collision efficiency, so that

$$J_{ij} = \alpha \beta_{ij} n_i n_j \tag{1}$$

where α denotes the collision efficiency (whose value lies between 0 and 1) and β_{ij} is the collision frequency between droplets of size i and j and n_i and n_j are the number concentrations of droplets of sizes i and j, respectively. The product $\alpha\beta_{ij}$ represents the number of successful collisions leading to flocculation and is, therefore, sometimes referred to as *flocculation frequency*. The creation of an aggregate of a given size necessarily means the loss of one or two aggregates of another size, hence, the changing number in a given size class can be represented by a population balance equation:

$$\frac{dn_p}{dt} = \frac{1}{2} \sum_{i+j=p} \alpha_{ij} \beta_{ij} n_i n_j - \sum_{i=1}^{\infty} \alpha_{ip} \beta_{ip} n_i n_p \tag{2}$$

The first term on the right-hand side denotes the formation of particles of size p due to aggregation of particles of sizes i and j (e.g., a single particle, $i = 1$, and an aggregate containing five particles, $j = 5$, will form an aggregate composed of six particles, $p = 6$). The factor of $\frac{1}{2}$ is to compensate for counting the same collisions twice. The second term represents the loss of particles of size p due to collision with other particles. Equation (2) summarizes the information we need to properly understand the kinetics of particle aggregation [i.e., $n_p(t)$], but, in practice, it is too complex to be of direct value. For each value of p in Eq. (2), there is a differential equation to be solved (assuming α_{ij} and β_{ij} are known). A realistic aggregate may contain several hundred particles, at which point the complexity is overwhelming. The useful theory arises from attempts to find a workable approximation to Eq. (2).

A. Smoluchowski Theory

The first attempt to describe the flocculation process in a population of particles was made by von Smoluchowski (8), who started by making several significant assumptions (listed in Table 2). Using these assumptions, Smoluchowski derived simple analytical expressions of collision frequency under perikinetic and orthokinetic conditions as shown in Eqs. (3) and (4), respectively:

$$\beta_{ij,\text{perikinetic}} = \frac{2kT}{3\mu} \tag{3}$$

$$\beta_{ij,\text{orthokinetic}} = \frac{4\gamma}{3} a^3 \tag{4}$$

where k is the Boltzmann constant, T is the temperature, μ is the viscosity of the continuous phase, a is the droplet diameter, and γ is the velocity

Table 2 Assumptions Used by von Smoluchowski in Deriving Particle Collision Rates

1. Particles are spherical after collision.
2. All collisions lead to immediate and complete coalescence (i.e., collision efficiency α equals unity and no colloidal or hydrodynamic forces exist).
3. There is no fracture of particles or aggregates.
4. Fluid motion is exclusively either diffusional or exclusively laminar shear.
5. Particles are of identical size.
6. Only two-particle collisions occur.

Source: Ref. 8.

gradient in the fluid. From Eq. (3), it can be seen that the collision frequency for perikinetic flocculation is independent of droplet size. To the contrary, for orthokinetic flocculation, Eq. (4) dictates that the collision frequency should increase with the cubic power of droplet size. Therefore, for fine droplets, applying a shear field may cause little change in the collision rate, whereas for larger droplets, there will be a large increase in the rate. The *total* number concentration (n_t) of the particles at any time t under orthokinetic conditions is given by the solution of the population balance equation (taking into account assumptions in Table 2) as

$$n_t = n_0 \exp\left(-\frac{4\gamma\phi t}{\pi}\right) \tag{5}$$

where n_0 is the initial total concentration of the particles and ϕ is the volume fraction of the particles. Equation (5) predicts that if the assumptions of this model are correct, then the number of particles is predicted to decrease exponentially with time at a rate proportional to volume fraction and shear rate.

Although Smoluchowski theory remains the basis for understanding particle collision rates, there remain fundamental problems. Most of the assumptions listed in Table 2 are violated in real systems and so the collision efficiency term α becomes an adjustable parameter without any theoretical basis. Several approaches have been taken to avoid one or more of the assumptions and, in particular, the methods of trajectory analysis have proved as a useful complementary approach to Smoluchowski theory.

B. Assumptions of Smoluchowski Theory

Smoluchowski theory remains the basis for understanding collision rates in sheared and unsheared emulsions. Several authors have made modifications to the Smoluchowski theory to avoid some of the assumptions violated in real systems. To some extent, it is possible to correct for these assumptions either with an entirely empirical collision efficiency or by using a more rigorous approach such as trajectory analysis (see Section II.C).

In this subsection, we will take the approach of Thomas et al. (9) and reevaluate Smoluchowski's assumptions and how other workers have attempted to deal with violations.

1. Particles Are Spherical in Shape After Collision

Although liquid emulsion droplets are spherical, we are often more concerned with their flocculation rather than calescence and, hence, in the

formation and properties of extended flocs. The Smoluchowski derivation for the rate of aggregation assumes that the particles remain spherical after collision; that is, the volumes of the two particles are additive, so that for an aggregate of N particles each of volume v and radius r, the total volume of the aggregate, V_N, and its radius, R_N, is given as

$$V_N = Nv \tag{6}$$
$$R_N = N^{1/3}a \tag{7}$$

However, experiments on shear-induced aggregation of solid particles have shown that the aggregates are not spherical but rather have an irregular structure (10–12) frequently described using fractal analysis (13,14). For a fractal aggregate, Eq. (7) is written as

$$R_N = N^{1/D}a \tag{8}$$

where D is the mass fractal dimension. If $D=3$ (as assumed in the Smoluchowski approach), then the structure is completely space filling. If $3 > D > 1$, then the volume of the aggregated structure is greater than the summed volume of the parts and so the collision radius of a fractal aggregate is always greater than that for an equivalent spherical aggregate. The lower the fractal dimension, the more open (porous) the aggregate structure. If $D=1$, the aggregated structure is linear, implying an aggregate consisting of a string of particles. Torres et al. (12) obtained a fractal dimension of $D=1.8$ for rapid coagulation under laminar shear flow and have shown that the floc structure (fractal dimension) was independent of shear rate. In addition, their experiments reveal that the floc structure is similar for perikinetic and orthokinetic aggregation, but the growth kinetics are different. Oles (11) showed that the initial growth phase of aggregation can be characterized by a fractal dimension of 2.1 and that later stages of growth yield $D=2.5$.

The presence of fractal flocs has important consequences for particle collision frequencies and efficiencies, as both of them are functions of particle size. In general, a decrease in fractal dimension enhances particle collision rates (15) (due to a larger collision profile) and increases collision efficiency (due to reduced viscous resistance to fluid flow; see Section II.C) (16). For fractal flocs, the orthokinetic collision frequency is similar to the expression developed by Smoluchowski [Eq. (4)] but uses the fractal aggregate radius from Eq. (8):

$$\beta_{ij} = \frac{4\gamma}{3} a^3 N^{3/D} \tag{9}$$

2. All Collisions Lead to Immediate and Complete Coalescence

The collision efficiency can take on a value less than 1 because of some repulsive interaction between the approaching particles. This may be due to colloidal forces or the hydrodynamic effects acting on the droplets. Colloidal forces are the result of the various noncovalent interactions that occur between particles. Each interaction decreases in magnitude in a specific manner with separation, and if particles move, they must do so either in response to or in opposition to the sum of forces acting at a given separation. This can be mapped as an interaction pair potential which describes the energy cost to move one particle from infinite separation to a given distance from a second, fixed particle and results from a summation of the various forces acting. One of the most commonly used pair potential is the DVLO potential (given as a sum of electrostatic repulsive and van der Waals attractive forces) and this is illustrated in Fig. 2.

At long separations, the interaction between the particles is effectively zero, but as they approach closer, the repulsive electrostatic interactions dominate over the attractive van der Waals forces and the particles are repulsed. At very close separations, the attractive forces dominate and the particles aggregate. (Note that for hard particles, there will be a very strong short-range steric repulsive force added to prevent coalescence.) The probability of two particles on a collision path approaching one another to the point of impact then depends on their kinetic energy and the potential energy surface over which they move. The important features of the interdroplet potential are the depth of the close separation energy well and the
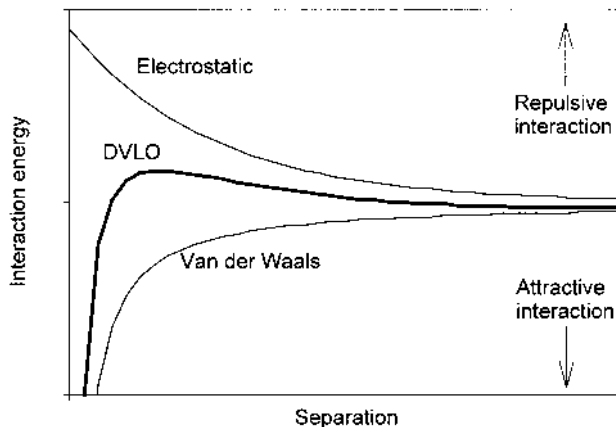
Figure 2 Diagrammatic representation of the DVLO interaction potential.

height of the intermediate separation barrier. Knowing these, it is possible to calculate a value for α under perikinetic conditions (17).

Hydrodynamic forces represent the energy required to make the fluid between the approaching particles to "get out of the way." They will act against particle approach and are thus repulsive forces. The relative movement of the fluid will also tend to cause approaching particles to rotate and take on a curved trajectory and miss one another. (Trajectory analysis is covered in more depth in Section II.C). Consequently, the presence of hydrodynamic forces will always reduce the collision frequency, sometimes by up to five orders of magnitude, compared to rectilinear trajectories (18). It is possible to calculate the effects numerically (7,18) and it is notable that the most dramatic reduction is in the case of orthokinetic flocculation—particularly with a wide disparity in particle sizes.

The structure of the flocs can affect the colloidal forces acting between them:

- **Impermeable porous flocs.** In the case of impermeable porous flocs (i.e., no passage of fluid through the floc), the collision efficiency (obtained from trajectory analysis) can be corrected for the fact that the van der Waals force between porous flocs is smaller than that of solid particles. This is so because the attractive force between two flocs can be considered to be that between the nearest primary particles, because the other particles in the floc are separated by too large a distance (19). Using this hypothesis, Kusters et al. (16) showed that collision efficiency between impermeable flocs decreases more rapidly with increasing particle size than that for solid particles.
- **Permeable porous flocs.** For permeable porous flocs, the hydrodynamic forces are less pronounced, due to penetration of fluid flow, resulting in higher values of collision efficiencies. The Debye shielding ratio, ξ, defined as

$$\xi = \frac{R}{\sqrt{\kappa}} \tag{10}$$

denotes the extent of passage of fluid flow, where R is the outer radius of floc and κ is the floc permeability. Porous flocs can also be represented using a shell–core model, which has an impermeable core with a completely permeable outer shell. The outer collision radius represents the distance within which another floc must approach for aggregation to occur. The inner impermeable core radius describes the drag experienced by the floc and corresponds to the hydrodynamic radius (R_H). With the knowledge of

hydrodynamic functions for hard spheres (20), the trajectories of the two colliding impermeable flocs are calculated and the outer radius is used to determine the point of contact. In this way, the influence of fluid flow penetration is accommodated in the collision efficiencies that follow from trajectory analysis (see Section II. C). Colloidal forces have not yet been satisfactorily incorporated in this model of floc structure. Nevertheless, the existing shell–core model has been shown to be in good qualitative agreement with the experimental results for aggregate growth under turbulent flow conditions (12,21).

More recently, experiments have demonstrated a nonuniform internal structure of the floc, in contrast to the uniform porosity assumed in the shell–core model (22). Collision efficiency of fractal flocs can be predicted by performing trajectory analysis, using the shell–core model described earlier (16). The floc structure is incorporated into the shell–core model using the Debye-shielding ratio that depends on the outer collision radius (which is a function of fractal dimension).

3. There Is No Fracture of Particles or Aggregates

Although neglected in Smoluchowski theory, in most systems flocs can break under the applied shear forces and the actual size distribution at any given time must account for both formation and destruction rates. The breakup of flocs occurs at a critical shear rate, at which the hydrodynamic force exceeds the attractive forces holding the flocs together; that is,

$$\frac{3}{2}\pi\mu R^2 \gamma \leq F_A \tag{11}$$

where R is the floc radius and F_A is the attractive force between the flocs (12). Two distinct modes of floc breakage have been reported in the literature under turbulent conditions: *floc erosion* and *floc fracture* (23). Floc erosion corresponds to the removal of primary particle from the surface of the floc and, in turbulent flow, predominates when floc size is smaller than the Kolmogorov scale. Floc fracture occurs in larger flocs and is due to the fluctuating motion of the fluid. Yeung and Pelton (24) showed experimentally that compact flocs are more susceptible to undergo surface erosion and less compact flocs are likely to fracture. Using a mean-field approach, Sonntag and Russel (25) developed a model for breakup that incorporates floc density in the form of fractal dimension. Their model was able to predict the shear-rate dependence of floc size, although their model neglected the rearrangement of flocs after breakup.

In practice, a flocculating system of particles, subjected to shear will eventually reach a steady state where the rate of floc fracture matches the rate of floc formation. The shear-rate dependence on the maximum stable floc size ($d_{F,\max}$) is given by (26,27):

$$d_{F,\max} = b\gamma^{-m} \tag{12}$$

where b and m are constants determined by the strength of the attractive forces and the internal floc structure, respectively. However, experimental results show that the effects of shear on maximum floc size could be quite complex. For example, restructuring of aggregates was observed at moderate shear rates (40–80 s^{-1}) but not at lower shear rates (28). Further, longer shearing times could lead to the formation of compact flocs (with higher fractal dimensions) due to restructuring (11,29). If the particle concentration is below a certain critical value, the maximum aggregate size depends only on shear rate, otherwise it is a function of both shear rate and concentration (30).

4. Fluid Motion Is Exclusively Laminar Shear

The approach taken by Smoluchowski was essentially a two-dimensional simplification of three-dimensional laminar flow. In most realistic cases, flow is three dimensional and it is more complex to define the motion of one particle relative to another. Camp and Stein (31) developed an alternative version of Eq. (4), replacing the velocity gradient with the root-mean-square velocity gradient (γ_{rms}), and although this approach is flawed (9), it retains considerable practical value. Root-mean-square velocity was related to the local rate of energy dissipation, ε, in laminar flow and the kinematic viscosity (υ) as

$$\gamma_{\mathrm{rms}} = \sqrt{\frac{\varepsilon}{\upsilon}} \tag{13}$$

Camp and Stein further extended this idea to turbulent flow by defining a bulk root-mean-square velocity ($\gamma_{\mathrm{rms}}^{*}$) in terms of the bulk rate of energy dissipation (ε^{*}). Incorporating the fractal dimensionality of realistic flocs, the collision rate is given as [see Eqs. (4) and (9)]

$$\beta_{ij} = 10.352\left(\frac{\varepsilon^{*}}{\upsilon}\right)^{1/2} a^3 N^{3/D} \tag{14}$$

5. Particles Are of Identical Size

Although fine liquid droplets are necessarily spherical, real emulsions are rarely monodisperse. Even for a hypothetical monodisperse emulsion,

Smoluchowski's assumption would soon be violated as doublets and triplets formed early in the aggregation process start to take part in further reactions. Solving for all of the rate constants in Eq. (2) is impractical for a large range of sizes; some authors have made assumptions instead about the allowable particle sizes:

- The allowable particle size must follow a predefined mathematical series (e.g., geometric, $n = 1, 2, 4, 8, 16,\ldots$). The loss of sensitivity is the cost for the reduced complexity of the calculations.
- The initial particle size distribution displays properties of self-preservation; that is, as the system aggregates, the entire distribution shifts to larger sizes but retains the same shape. In such instances, a correction factor can be introduced to collision efficiency to account for polydispersity (32).

6. Only Two-Particle Collisions Occur

As systems become progressively more concentrated, this assumption becomes less valid; however, the theoretical demands of multibody collisions have not yet been adequately incorporated into Smoluchowski theory.

Despite its limitations, Smoluchowski theory, particularly as modified by Camp and Stein [Eq. (13)], remains the basis for understanding droplet collision behavior. However, as we have seen, it has many limitations restricting its applicability and many of the approaches to deal with its assumptions are largely empirical. A more detailed and fundamental approach can be gained through trajectory analysis.

C. Trajectory Analysis

The limitations of Smoluchowski theory are typically addressed through the adjustable parameter α, the collision efficiency. This approach is broadly macroscopic and allows no detailed description of the nature of the interactions taking place. If we know all of the forces involved, it would be theoretically possible to simulate the aggregation process through computer simulation (Monte Carlo or colloidal dynamics). However, it is often preferred to consider only two-body interactions in more depth. Trajectory analysis is a powerful, although somewhat complex, tool to understand the motion of one particle relative to another, but it is only suitable for two-body interactions and, thus, is only quantitatively valid for very dilute suspensions ($\phi \ll 0.01$). We shall introduce some of the important conclusions from trajectory analysis in the following paragraphs, but for a more in
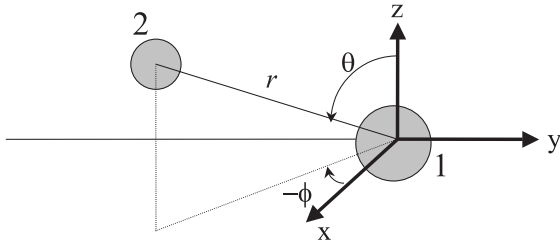
Figure 3 Diagram showing the axis system used for trajectory analysis of the interaction between a reference sphere (1) and a collision sphere (2). The flow direction is along y axis and the velocity gradient is along the x axis.

depth discussion, the reader is advised to refer to Van de Ven's book (33) and a recent review by Vanni and Baldi (34).

Trajectory analysis is a method to determine the path of interaction of two spheres in a fluid flow. It is assumed that one of the spheres is fixed at the origin (reference sphere) and the relative trajectory of the other sphere (collision sphere) is then calculated (Fig. 3). Another key assumption is that the interaction forces act along the line joining the centers of the two spheres and are balanced by the component of the hydrodynamic force in that direction. The equations governing the trajectories of the two particles in a *simple laminar shear flow* are given by Vanni and Baldi (34):

$$\frac{dr}{dt} = \gamma r(1 - A)\sin^2\theta\sin\phi\cos\phi + \frac{CE_{\text{int}}}{6\pi\mu a_1} \tag{15}$$

$$\frac{d\theta}{dt} = \gamma(1 - B)\sin\theta\cos\theta\sin\phi\cos\phi \tag{16}$$

$$\frac{d\phi}{dt} = \gamma\left(\cos^2\phi - \frac{B}{2}\cos 2\phi\right) \tag{17}$$

where γ is the shear rate and the angles θ and ϕ, and the distance r represent the relative positions of the particles in radial coordinates (see Fig. 3). F_{int} is the interparticle pair potential, and A, B, and C are hydrodynamic mobility functions which depend on the dimensionless center distance $r^* = r/a_1$ and on the size ratio $\lambda = a_2/a$ where a is the particle radius and subscripts 1 and 2 refer to the reference and collision spheres, respectively. Approximate
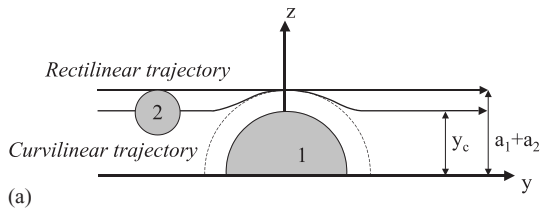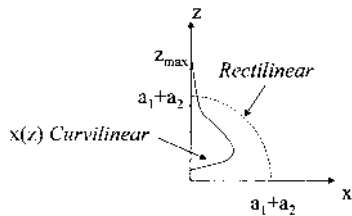
Figure 4 (a) Limiting trajectories of the interaction of a collision sphere (2) with a reference sphere (1). The broken circle indicates the region through which sphere 2 must pass to collide with sphere 1. The rectilinear trajectory starts at the minimum distance from the origin for sphere 2 to miss sphere 1 using Smoluchowski assumptions (i.e., rectilinear trajectories). The curvilinear trajectory starts at the minimum distance from the origin for sphere 2 to miss sphere 1 when hydrodynamic forces are included (i.e., curvilinear trajectories). Note that $y_c < a_1 + a_2$ when hydrodynamic forces act, so fewer particles in the flux will collide. Again, the y-x plane is the flow-gradient plane. (b) Collision surfaces calculated from trajectory analysis. The surface marked rectilinear is that predicted from the Smoluchowski (i.e., no colloidal forces acting). The surface marked curvilinear is a sample result that may occur when colloidal and hydrodynamic forces are taken into account. (Adapted from Ref. 34.)

expressions for the hydrodynamic (34) and the interparticle pair potential functions (35) are available in the literature.

The trajectory of the collision sphere is determined by numerically integrating Eqs. (15–17) (Fig. 4a). The numerical integration requires knowledge of the initial position and velocity of the particle. The collision sphere is made to approach the reference sphere from an infinite distance (at least 10 particle separations) and can have 3 possible outcomes. It can undergo collision (i.e., primary coagulation: $r/a_1 < 1 + a_2/a_1 + \varepsilon$,

where ε is a predetermined parameter set in the numerical integration) or orbit around the reference sphere (i.e., secondary coagulation: $\phi > \pi/2$) or simply depart to infinity without contacting the reference sphere ($y/a_1 > 10$). The calculation is repeated from a number of starting positions and a collision surface is mapped.

A collision surface can be calculated as those starting positions for fluid flow that would result in particle collision (Fig. 4b). If interparticle forces and hydrodynamic forces are neglected, then the collision sphere would follow the stream lines of the simple shear flow (i.e., rectilinear trajectories). In such as case, a collision occurs for all particles that move toward the reference particle within the cylinder defined by $a_1 + a_2$. If the distance of approach is greater than this distance, the particles will miss each other. The collision surface in Smoluchowski theory is a circle, whose radius is defined by the distance of limiting trajectory from the origin (i.e., $a_1 + a_2$) (Fig. 4b).

The flux is given by

$$J = \int dJ = \int_s NvZ(s)\,ds \tag{18}$$

where N is the number of particles crossing the collision surface $Z(s)$ and v represents the particle velocity. Taking $Z(s)$ as a circle of radius $a_1 + a_2$, simple integration yields the Smoluchowski flux equation:

$$J_0 = \frac{4}{3}\gamma N(a_1 + a_2)^3 \tag{19}$$

[Note Eq. (19) is a general case of Eq. (4) for dissimilar particle sizes.] When only hydrodynamic forces are acting, then the trajectories become curvilinear (Fig. 4a) and the definition of the collision surface is no longer obvious (Fig. 4b). The hydrodynamic forces cause the collision particle to roll past the reference particle and miss even though it started within the $a_1 + a_2$ limit for collision if the path had been rectilinear (Fig. 4a; $y_c < a_1 + a_2$). Note that the trajectory is symmetric about the y axis; that is, the positions of the collision particle at the upstream and downstream region are mirror images of each other. The full problem of incorporating colloidal and hydrodynamic forces into trajectory analysis has been solved by various authors (36–39) to calculate the collision surface. The collision surface in this case could be quite irregular, as shown in Fig. 4b. In this case, the flux is given by

$$J = 4\gamma N \int_0^{z_{max}} xz(x)\,dx \tag{20}$$

Note that in this case the trajectories are asymmetrical about the y axis, because the collision sphere spends a much longer time in the vicinity of the reference sphere due to the colloidal interaction force. In addition, the curvilinear trajectory in Fig. 4b extends beyond the Smoluchowski limit of $a_1 + a_2$, suggesting that some of the particles may stick in the downstream region after crossing the x-z plane.

The collision efficiency is then given by the ratio of Eqs. (19) and (20) (i.e., the ratio between actual collision rates incorporating all forces and the ideal collision rate with no forces acting):

$$\alpha = \frac{3}{(a_1 + a_2)^3} \int_0^{z_{\max}} xz(x)\, dx \tag{21}$$

By this method, it is possible to directly calculate the adjustable parameter, α, in Smoluchowski theory from known physical properties of the system. This formulation of trajectory analysis assumes diffusional mobility of the particles is insignificant compared to shear. For particle aggregation under shear flow, Swift and Friedlander (40) showed that the Brownian and bulk convective motion could be treated independent of each other and thus merely added to determine the combined effect; however van de Ven and Mason (41) showed that the additive assumption is incorrect when Brownian effects were large compared to shear forces [i.e., at very low Pe (the Peclet number)].

This analysis is strictly for solid droplets and there are some important differences for fluid particles, which can deform due to the forces acting. The hydrodynamic functions for interacting droplets depend not only on the size ratio of the two droplets and the dimensionless interdroplet distance but also on the droplet–medium viscosity ratio because the particles can deform somewhat to absorb the hydrodynamic stress (42,43).

III. EXPERIMENTS IN FOOD SYSTEMS

Finally, we shall consider some of the experimental studies on food emulsion stability that have considered shear as a variable. Most of the orthokinetic studies in food emulsions have been done in fairly concentrated emulsions (10–30 wt%) and will be reviewed first. Later, we will examine recent work by the Leeds group that has developed a particle capture technique to study interactions between two colloidal particles in a laminar shear field (44).

A. Orthokinetic Studies on Concentrated Emulsions

In experimental studies on shear-induced aggregation of concentrated food emulsions, the measured parameter almost always has been the change in droplet size distribution. The variation in droplet size distributions due to coalescence/flocculation is transformed into a coalescence rate constant or coalescence efficiency, to quantify the effect of shear. In some cases, viscosity is used as a proxy for particle aggregation. Typical results show a sigmoidal function for particle size in time for emulsion destabilization under shear (Fig. 5). In the first portion of the graph, there is no change because the primary droplets have a very low reactivity. However, once a few droplets do aggregate, then the rate of reaction increases with particle size (particularly important for fractal flocs). However, large flocs are eroded (or fractured) by the velocity gradient, and as the size increases, this process will match the rate of aggregation and reach an equilibrium value of particle size. This equilibrium may change if the shear rate is changed or stopped.

1. Emulsions Containing Liquid Droplets

Van Boekel and Walstra studied the effect of laminar Couette flow on the stability of paraffin oil-in-water emulsions stabilized by various surfactants. The experimental rate constant for coalescence (k_{exp}) was taken as the slope of a linear fit to a plot of droplet size with time (on a semilog scale). The theoretical rate constant of coalescence was derived from Smoluchowski rate equation

$$\frac{dn_t}{dt} = -k_{theory}n_t \tag{22}$$
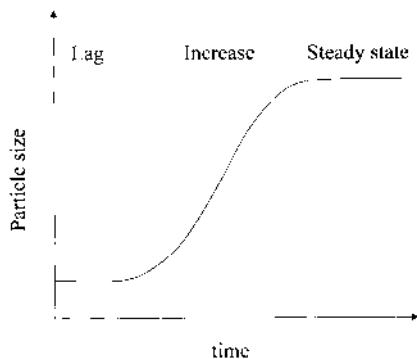
Figure 5 Schematic diagram showing typical changes in particle size for an emulsion undergoing orthokinetic flocculation.

which is obtained by differentiating Eq. 5, where

$$k_{\text{theory}} = \frac{4\gamma\varphi}{\pi} \tag{23}$$

They quantified the effect of shear in terms of coalescence efficiency defined as the ratio of k_{exp} to k_{theory}. The orthokinetic studies showed that emulsions that were stable at rest were also stable during Couette flow (45,46). In addition, they observed that in emulsions that were unstable at rest, Couette flow did not have any significant influence on the rate of coalescence. Increasing the shear rate would increase the frequency of collisions, but these authors argued that it would simultaneously decrease the duration of encounters (i.e., collision efficiency decreased with shear rate in Couette flow). Attempts were made by these authors to increase the orthokinetic collision efficiency through the addition of NaCl, but the emulsions remained resistant to shear-induced coalescence. This led them to suggest that the duration of an encounter is more important than the number of encounters *per se*. In addition, the authors performed trajectory analysis to calculate the collision efficiency for doublet formation, which was much higher than the measured value.

In contrast, under turbulent flow, a dramatic increase in aggregation rate after a few larger, more reactive particles were formed was seen by Dickinson and Williams (47) in a study of the orthokinetic stability of protein-stabilized emulsions. They observed that there was a sharp divergence in d_{32} after an initial lag phase and defined a characteristic destabilization time at the maximum rate of increase in the mean droplet diameter. They proposed the sudden destabilization in terms of an increasing reactivity of droplets with increasing droplet size (α is a strong function of particle diameter), similar to the critical phenomenon in a sol–gel transition (48) and used a two-parameter model to describe the process:

$$\frac{dn_t}{dt} = k_d n_t - k_c n_t^2 \tag{24}$$

where k_d and k_c are the rate constants for disruption and coalescence, respectively. The coalescence rate constant was assumed to depend on droplet size and fractal dimension [see Eq. (9)]. They further invoked a minimum droplet size breakup criterion [see Eq. (11)]. This model showed that a fractal dimension $D \sim 2$ was required to match the experimental data, which is in reasonable agreement with other orthokinetic studies. These and other workers argued that attractive colloidal forces make emulsions more vulnerable to shear-induced aggregation. For example, adjusting the

pH toward the *pI* of the protein-stabilizing layer (47) and adding calcium to a caseinate-stabilized system (49,50) have all been shown to increase the susceptibility to orthokinetic destabilization. Furthermore, adding a small amount of small-molecule surfactant to a protein-stabilized emulsion increased the orthokinetic destabilization rate without causing significant displacement (51,52). (It was argued that the increased membrane fluidity caused by adsorbed surfactant was responsible.) On the other hand, increased amounts of interfacial protein (presumably forming a thicker layer) decreased the susceptibility to orthokinetic destabilization (50).

As well as increasing the rate of orthokinetic aggregation, increased shear rates can limit the maximum (equilibrium particle size) achieved by increasing the rate of aggregate fracture. For example, Schokker and Dalgleish (50) showed that reciprocal maximum particle diameter was proportional to the shear rate used for a caseinate-stabilized emulsion [i.e., $m = -1$ in Eq. (11)]. Again, by increasing the magnitude of the attractive forces between aggregated particles, which oppose the shear-induced stresses on the floc [e.g., by adding calcium to a caseinate stabilized emulsion (49,50), the final floc size achieved can be increased].

2. Emulsions Containing Semicrystalline Droplets

For liquid-oil emulsions, aggregation is generally due to interactions between the surface layers and the oil composition itself has limited effect. However, in many emulsions of practical interest, the oil phase may be partially crystalline at usage temperatures (46). The crystals can form as spikes at the droplet interface and the crystalline droplets are more reactive toward other semisolid droplets (53). The fat crystals in one droplet induce instability by penetrating the thin film between two approaching droplets and allowing liquid oil to flow out around the interaction site to reinforce the link. This phenomenon is known as partial coalescence because although there is mixing of the oil from two droplets, the crystal network is sufficient to maintain the doublet shape. Completely solid or liquids cannot partially coalesce, as they lack the required liquid or solid fat fraction, respectively. Because partial coalescence requires direct droplet–droplet contact, it would be reasonably expected to be highly dependent on shear rate. Walstra (1) argued that the applied shear (a) increases the collision rate, (b) pushes the colliding droplets closer together so the protruding crystal size approaches the film thickness, and (c) the hydrodynamic forces between the droplets causes the droplets to roll around one another, increasing the probability that a suitable protruding crystal will be able to penetrate the interdroplet membrane.

Partial coalescence is particularly important in milk fat emulsions because butter oil has a wide melting range and under storage conditions ($\sim 5^\circ$C) is semisolid. Milk fat globules are quite stable to coalescence when at rest (except slow creaming). However, it has been shown that liquid milk fat globules are unstable under Couette flow (46), probably because the increased collision rate for the large droplets is sufficient to enhance the rate of partial coalescence. Van Boekel and Walstra (46) observed that the coalescence efficiency remained constant with increasing laminar shear rate, indicating that the rate of coalescence was proportional to the encounter frequency and not the product of frequency and duration, as suggested for liquid-oil emulsions (see above).

Minor components in the fat are very capable of affecting the orientation of crystals to the surface and hence the orthokinetic stability of the semicrystalline emulsion. Davies and others (54) studied the shear stability of partly crystalline triglyceride droplets stabilized with sodium caseinate. The emulsions were quiescently stable but had clear stress limits that, if exceeded, would quickly lead to emulsion destabilization. The magnitude of these stress limits decreased with increasing solid fat content and with increasing added monoglycerides. The monoglycerides were believed to both weaken the protein coat of the droplets and act as a template favoring crystal growth/accumulation at the surface (55). Hinrichs and Kessler (56) also noted the presence of a critical limit in the strain rate required to destabilize milk fat globules. The magnitude of this critical limit decreased linearly with fat volume fraction and increased with solid fat content.

B.   Two-Particle Aggregation Under Shear

The macroscopic approaches used in the above-described studies, although practical, does not provide quantitative information regarding the interplay of colloidal and hydrodynamic forces. Recently, the role of such forces in food systems was studied by the Leeds Group using a colloidal particle scattering technique (57–60). In this technique, the capture of one droplet moving in a shear field by a second (fixed) droplet was observed. This microscopic approach yields trajectories of the moving droplet, which were then compared with computer simulations of the trajectories (similar to the trajectory analysis discussed in Section II. C) to obtain quantitative information about dynamic colloidal interactions. In addition, the capture efficiency (which is qualitatively similar to collision efficiency described in Section III. A) was determined, which was defined as the ratio of number of collisions leading to the formation of a doublet to the total number of trials.

The particles used in the particle-scattering technique were latex and emulsion droplets, coated with protein emulsifiers including sodium caseinate, β-casein, and α_{s1}-casein. They observed that in caseinate-stabilized emulsions, the capture efficiency was highest at the isoelectric point (pH = 4.7) (60), as expected from the macroscopic studies (e.g., Ref. 47). To achieve a good fit with the experimental data, it was necessary to develop a theory for the colloidal forces acting between the droplets [see Eq. (15)]. These workers initially used a DLVO potential (as shown in Fig. 2) with an additional DeGennes steric repulsive interaction but this agreed poorly with the data. Further, this model did not predict the observed upstream sticking of the mobile particle to the fixed particle. Only by incorporating a pH-dependent tangential interparticle force, which they hypothesized could arise from entanglement of the adsorbed polymer layers at the interface, were they able to successfully predict the variation of capture efficiency with pH. When ionic strength was included as an additional parameter, the behavior was complex. At lower pH (< 5.2), sticking probability was sensitive to lower values of ionic strengths ($< 0.2\,M$), indicating the importance of charged interactions in shear-induced aggregation. At higher ionic strength ($=0.5\,M$), it was unclear as to why the capture efficiency would decrease dramatically.

IV. CONCLUSIONS

We are interested in the changing structure and functionality of food emulsions over long periods of quiescent storage and short periods of varying flow during manufacture and use. The forces acting on the droplets in each case and so the behavior of the emulsions can be very different. Although the basic Smoluchowski approach is often invalid in sheared systems because of the strong effect of hydrodynamic forces, it is possible to use modified theories, particularly in combination with trajectory analysis, to give good predictions of collision rates in dilute emulsions. However, as concentration is increased, the theoretical assumptions are violated and the theories may prove unreliable. Furthermore, the colloidal interaction potential needed for trajectory analysis are difficult to know precisely a priori for a realistic system and can easily become a hidden fitting parameter. The particle scattering approach taken by Dickinson and others (44,57–60) provides a more experimental approach to verify the behavior of pairs of particles, although the possibility of multibody interactions at higher concentrations cannot be considered.

Experimental study of emulsion destabilization in flow is also challenging. Modern rheometers are ideal for providing controlled flow rates

in a fluid, but the characterization of the response of the suspension is more complex. Increased viscosity is a sensitive measure of droplet flocculation (but not to coalescence) and is relatively easy to measure in situ if the rheometer is also used to generate the fluid flow (e.g., Ref. 54). However, although it is possible to infer aggregate structure from rheological measurements, this is an indirect approach. Removing samples from the flow for analysis by conventional light scattering (48) or microscopy (61–64) is possible, but this has the disadvantage of changing the balance of forces acting and possibly the structures present (65). Some authors have combined rheometers and light-scattering instruments to study aggregation under shear, but this is necessarily restricted to dilute systems (12,28,66). Other methods of particle sizing suited to concentrated emulsions, particularly ultrasonic spectroscopy, may be more suited to the study of suspension structure under shear (61,64). Hamberg and others (67) recently used several methods to study the changes in the structure of latex particles covered with whey protein in shear flow. First, by using fluid gelatine solution as the continuous phase, they were able to easily fix samples removed from the rheometer for optical microscopy. Second they used a four-roll mixer to generate a region of laminar shear flow between the rollers and imaged this flow using a confocal laser scanning microscope.

In conclusion, we can expect that the fluid flow to drastically effect emulsion structure and that studies on quiescent systems need not apply when the mixture is sheared. The effects can be both complex and unexpected.

REFERENCES

1. P. Walstra, Emulsion stability, in *Encyclopedia of Emulsion Technology* (P. Becher, ed.), Marcel Dekker, New York, 1996, Chap. 1.
2. H. A. Barnes, Rheology of emulsions—a review, *Colloids Surfaces A* 91, 89–95 (1994).
3. J. F. Steffe, *Rheological Methods in Food Process Engineering*, 2nd ed., Freeman Press, East Lansing, MI, 1996.
4. P. Walstra, Principles of emulsion formation, *Chem. Eng. Sci.* 48, 333–349 (1993).
5. E. Dickinson, Proteins at interfaces and in emulsions. Stability, rheology and interactions, *J. Chem. Soc. Faraday Trans.* 94, 1657–1667 (1998).
6. V. G. Levich, *Physicochemical Hydrodynamics*, Prentice-Hall, Englewood Cliffs, NJ, 1962.
7. M. Y. Han and D. F. Lawler, The (relative) insignificance of **g** in flocculation, *J. Am. Water Works Assoc.* 84, 79–91 (1992).

8. M. Smoluchowski, Verusch einer Mathematischen Theorie der Koagulationskinetik Kolloider Lösungen, *Z. Phys. Chem.* 92, 129–168 (1917).

9. D. N. Thomas, S. J. Judd, and N. Fawcett, Flocculation modeling: A review, *Water Res.* 33, 1579–1592 (1999).

10. R. C. Klimpe and R. Hogg, Effects of flocculation conditions on agglomerate structure, *J. Colloid Interf. Sci.* 113, 121–131 (1986).

11. V. Oles, Shear-induced aggregation and breakup of polystyrene latex particles, *J. Colloid Interf. Sci.* 154, 351–358 (1992).

12. F. E. Torres, W. B. Russel, and W. R. Schowalter, Floc structure and growth kinetics for rapid shear coagulation of polystyrene colloids, *J. Colloid Interf. Sci.* 142, 554–574 (1991).

13. B. B. Mandelbrot, *The Fractal Geometry of Nature*, W. H. Freeman, San Francisco, 1982.

14. P. Meakin, Fractal aggregates, *Adv. Colloid Interf. Sci.* 28, 249–331 (1988).

15. Q. Jiang and B. E. Logan, Fractal dimensions of aggregates determined from steady state size distributions, *Environ. Sci. Technol.* 25, 2031 (1991).

16. K. A. Kusters, J. G. Wijers, and D. Thoenes, Aggregation kinetics of small particles in agitated vessels, *Chem. Eng. Sci.* 52, 107–121 (1997).

17. N. Fuchs. Über die stabilität und aufladung der aerosole, *Z. Phys.* 89, 736–743 (1934).

18. D. F. Lawler, Physical aspects of flocculation: From microscale to macroscale, *Water Res.* 27, 164–180 (1993).

19. B. A. Firth and R. J. Hunter, Flow properties of coagulated colloidal suspensions. I. Energy dissipation in the flow units, *Colloid Interf. Sci.* 57, 248–256 (1976).

20. P. M. Adler, Heterocoagulation in shear flow, *J. Colloid Interf. Sci.* 83, 106–115 (1981).

21. K. A. Kusters, The influence of turbulence on aggregation of small particles in agitated vessel, Ph. D. thesis, Eindhoven University of Technology, Eindhoven, 1991.

22. R. C. Sonntag and W. B. Russel, Structure and breakup of flocs subjected to fluid stresses 1. Shear experiments, *J. Colloid Interf. Sci* 113, 399–413 (1986).

23. K. Muhle, Floc stability in laminar and turbulent flow, in *Coagulation and Flocculation: Theory and Applications* (B. Dobias, ed.), Marcel Dekker, New York, 1993, pp. 355–390.

24. A. K. C. Yeung and R. Pelton, Micromechanics: A new approach to studying the strength and break-up of flocs, *J. Colloid Interf. Sci.* 184, 579–585 (1996).

25. R. C. Sonntag and W. B. Russel, Structure and breakup of flocs subjected to fluid stresses 2. Theory, *J. Colloid Interf. Sci.* 115, 378–389 (1986).

26. J. C. Flesch, P. T. Spicer, and S. E. Pratsinis, Laminar and turbulent shear-induced flocculation of fractal aggregates, *AIChE J.* 45, 1114–1124 (1999).

27. A. A. Potanin, On the mechanism of aggregation in the shear flow suspensions, *J. Colloid Interf. Sci.* 145, 140 (1991).

28. C. Selomulya, R. Amal, G. Bushell, and T. D. Waite, Evidence of shear rate dependence on restructuring and break-up of latex aggregates, *J. Colloid Interf. Sci.* 236, 67–77 (2001).

29. P. T. Spicer and S. E. Pratsinis, Shear-induced flocculations: The evolution of floc structure and the shape of the size distribution at steady state, *Water Res.* 30, 1049–1056 (1996).

30. T. Serra and X. Casamitjana, Effect of shear and volume fraction on the aggregation and breakup of particles, *AIChE J.* 44, 1724–1730 (1998).

31. T. R. Camp and P. C. Stein, Velocity gradients and internal work in fluid motion, *J. Boston Soc. Civil Eng.* 30, 219–237 (1943).

32. V. Mishra, S. M. Kresta, and J. H. Masliyah, Self-preservation of the drop size distribution function and variation in the stability ratio for rapid coalescence of a polydisperse emulsion in a simple shear field, *J. Colloid Interf. Sci.* 197, 57–67 (1998).

33. T. G. M. Van der Ven, *Colloidal Hydrodynamics*, Academic Press, London, 1989.

34. M. Vanni and G. Baldi, Coagulation efficiency of colloidal particles in shear flow, *Adv. Colloid Interf. Sci.* 97, 151–177 (2002).

35. J. N. Israelachvili, *Intermolecular and Surface Forces*, Academic Press, London, 1992.

36. D. L. Feke and W. R. Schowalter, The effect of Brownian diffusion on shear-induced coagulation of colloidal dispersions, *J. Fluid Mech.* 133, 17 (1983).

37. D. L. Feke and W. R. Schowalter, The influence of Brownian diffusion on binary flow-induced collision rates in colloidal dispersions, *J. Colloid Interf. Sci.* 106, 203 (1985).

38. T. G. M. Van der Ven and S. G. Mason, The microrheology of colloidal dispersions. VII. Orthokinetic doublet formation of spheres, *Colloid Polym. Sci.* 255, 468–479 (1977).

39. G. R. Zeichner and W. R. Schowalter, Use of trajectory analysis to study stability of colloidal dispersions, *AIChE J.* 23, 243–254 (1977).

40. D. L. Swift and S. K. Friedlander, The coagulation of hydrosols by Brownian motion and laminar shear flow, *J. Colloid Sci.* 19, 621–647 (1964).

41. T. G. M. Van der Ven and S. G. Mason, The microrheology of colloidal dispersions. VIII. Effect of shear on perikinetic doublet formation, *Colloid Polym. Sci.* 255, 794 (1977).

42. H. Wang, A. Z. Zinchenko and R. H. Davis, The collision rate of small drops in linear flow fields, *J. Fluid Mech.* 265, 161–188 (1994).

43. A. Z. Zinchenko and R. H. Davis, Collision rates of spherical drops of particles in a shear flow at arbitrary Peclet numbers, *Phys. Fluid* 7, 2310–2327 (1995).

44. B. S. Murray, E. Dickinson, J. M. McCarney, P. V. Nelson, M. Whittle, Observation of the dynamic colloidal interaction forces between casein-coated latex particles, *Langmuir* 14, 3466–3469 (1988).

45. M. A. J. S. van Boekel and P. Walstra, Effect of Couette flow on stability of oil-in-water emulsions, *Colloids Surfaces* 3, 99–107 (1981).

46. M. A. J. S. van Boekel and P. Walstra, Stability of oil-in-water emulsions with crystals in the disperse phase, *Colloids Surfaces* 3, 109–118 (1981).
47. E. Dickinson and A. Williams, Orthokinetic coalescence of protein-stabilized emulsions, *Colloids Surfaces A* 88, 317–326 (1994).
48. A. Lips, T. Weatbury, P. M. Hart, I. D. Evans, and I. J. Campbell, On the physics of shear-induced aggregation in concentrated food emulsions, in *Food Colloids and Polymers: Stability and Mechanical Properties* (P. Walstra, ed.), Royal Society of Chemistry, Cambridge, 1993, pp. 31–44.
49. E. Dickinson and E. Davies, Influence of ionic calcium on stability of sodium caseinate emulsions, *Colloids Surfaces B* 12, 203–212 (1999).
50. E. P. Schokker and D. G. Dalgleish, Orthokinetic flocculation of caseinate-stabilized emulsions: Influence of calcium concentration, shear rate and protein content, *J. Agric. Food Chem.* 48, 198–203 (2000).
51. E. Dickinson, G. Iverson, and J. Chen, Interfacial interactions, competitive adsorption and emulsion stability, *Food Struct.* 12, 135–146 (1993).
52. E. Dickinson, R. K. Owusu, and A. Williams, Orthokinetic destabilization of a protein stabilized emulsion by a water soluble surfactant, *J. Chem. Soc. Faraday Trans.* 89, 865 (1993).
53. D. Rousseau, Fat crystals and emulsion stability—a review, *Food Res. Int.* 33, 3–14 (2000).
54. E. Davies, E. Dickinson, and R. D. Bee, Shear stability of sodium caseinate emulsions containing monglyceride and triglyceride crystals, *Food Hydrocolloids* 14, 145–153 (2000).
55. E. Davies, E. Dickinson, and R. D. Bee, Orthokinetic destabilization of emulsions by saturated and unsaturated monoglycerides, *Int. Dairy J.* 11, 827–836 (2001).
56. J. Hinrichs and H. G. Kessler, Fat content of milk and cream and effects on fat globule stability, *J. Food Sci.* 62, 992–995 (1997).
57. H. Casanova, J. Chen, E. Dickinson, B. S. Murray, P. V. Nelson, and M. Whittle, Dynamic colloidal interactions between protein-stabilized particles—experiment and simulation, *Phys. Chem. Chem. Phys.* 2, 3861–3869 (2000).
58. E. Dickinson, B. S. Murray, M. Whittle, and J. Chen, Dynamic interactions between adsorbed protein layers from colloidal particle scattering in shear flow, *Food Colloids: Fundamentals of Formulation* (R. Miller, ed.), Royal Society of Chemistry, Cambridge, 2000, pp. 37–51.
59. M. G. Semenova, J. Chen, E. Dickinson, B. S. Murray, and M. Whittle, Sticking of protein-coated particles in a shear field, *Colloid Surfaces B* 22, 237–244 (2001).
60. M. Whittle, B. S. Murray, J. Chen, and E. Dickinson, Simulation and experiments on colloidal particle capture in a shear field, *Langmuir* 16, 9784–9791 (2000).
61. R. Chanamai, N. Hermann, and D. J. McClements, Ultrasonic spectroscopy study of flocculation and shear-induced floc disruption in oil-in-water emulsion, *J. Colloid Interf. Sci.* 204, 268–276 (1998).

62. H. Mousa, W. Agterof, and J. Mellema, Experimental investigation of the orthokinetic coalescence efficiency of droplets in simple shear flow, *J. Colloid Interf. Sci.* 240, 340–348 (2001).

63. A. Nandi, D. V. Khakhar, and A. Mehra, Coalescence in surfactant-stabilized emulsions subjected to shear flow, *Langmuir* 17, 2647–2655 (2001).

64. S. A. Vanapalli and J. N. Coupland, Emulsions under shear—the formation and properties of partially coalesced lipid structures, *Food Hydrocolloids* 15, 507–512 (2001).

65. E. P. Schokker and D. G. Dalgleish, The shear-induced destabilization of oil-in-water emulsions using caseinate as emulsifier, *Colloids Surfaces A* 145, 61–69 (1988).

66. W. Xu, A. Nikolov, D. T. Wasan, A. Gonsalves, and R. P. Borwankar, Fat particle structure and stability of food emulsions, *J. Food Sci.* 63, 183–188 (1998).

67. L. Hamberg, P. Walkenstrom, M. Stading, and A. M. Hermansson, Aggregation, viscosity measurements and direct observation of protein coated latex particles under shear, *Food Hydrocolloids* 15, 139–151 (2001).